

Retraction

Retracted: Operational Status Monitoring and Fault Diagnosis System of Transformer Equipment

Wireless Communications and Mobile Computing

Received 13 September 2023; Accepted 13 September 2023; Published 14 September 2023

Copyright © 2023 Wireless Communications and Mobile Computing. This is an open access article distributed under the Creative Commons Attribution License, which permits unrestricted use, distribution, and reproduction in any medium, provided the original work is properly cited.

This article has been retracted by Hindawi following an investigation undertaken by the publisher [1]. This investigation has uncovered evidence of one or more of the following indicators of systematic manipulation of the publication process:

- (1) Discrepancies in scope
- (2) Discrepancies in the description of the research reported
- (3) Discrepancies between the availability of data and the research described
- (4) Inappropriate citations
- (5) Incoherent, meaningless and/or irrelevant content included in the article
- (6) Peer-review manipulation

The presence of these indicators undermines our confidence in the integrity of the article's content and we cannot, therefore, vouch for its reliability. Please note that this notice is intended solely to alert readers that the content of this article is unreliable. We have not investigated whether authors were aware of or involved in the systematic manipulation of the publication process.

Wiley and Hindawi regrets that the usual quality checks did not identify these issues before publication and have since put additional measures in place to safeguard research integrity.

We wish to credit our own Research Integrity and Research Publishing teams and anonymous and named external researchers and research integrity experts for contributing to this investigation.

The corresponding author, as the representative of all authors, has been given the opportunity to register their agreement or disagreement to this retraction. We have kept a record of any response received.

References

- [1] G. Yuan and S. Zhang, "Operational Status Monitoring and Fault Diagnosis System of Transformer Equipment," *Wireless Communications and Mobile Computing*, vol. 2022, Article ID 4684480, 8 pages, 2022.

Research Article

Operational Status Monitoring and Fault Diagnosis System of Transformer Equipment

Guijun Yuan  and Songtao Zhang 

Inner Mongolia Power (Group) Co., Ltd., Xilingol Electric Power Bureau, Xilinhaote, Neimenggu 026000, China

Correspondence should be addressed to Songtao Zhang; 201804319@stu.ncwu.edu.cn

Received 1 June 2022; Revised 16 June 2022; Accepted 22 June 2022; Published 16 July 2022

Academic Editor: Aruna K K

Copyright © 2022 Guijun Yuan and Songtao Zhang. This is an open access article distributed under the Creative Commons Attribution License, which permits unrestricted use, distribution, and reproduction in any medium, provided the original work is properly cited.

In order for valuable distribution transformer data to provide a potential solution for monitoring abnormal conditions, the authors propose a data-driven abnormal state monitoring data acquisition algorithm for distribution network transformers. The algorithm can alert operators and maintenance personnel of abnormal conditions in a timely manner. In the proposed algorithm, the Spearman rank correlation coefficient is used to display the correlation between phase currents, and its t statistic is used to determine whether there is an abnormality in the determined data collection based on hypothesis testing. Finally, the effectiveness of the proposed algorithm is verified by using the actual data collected from the power grid, and the characteristics of normal and abnormal conditions are analyzed separately. Sensitivity analyses were performed for different significance levels and sampling rates to consider their impact on monitoring results. The application results show that the power grid recovered a total of 12.98 million yuan from 136 households with a power consumption of 17.57 GWh, proving the practicability of the algorithm. *Conclusion.* The application in the actual power system is given, and the feasibility of the algorithm is proved.

1. Introduction

Driven by modern technology, the power grid is becoming more and more intelligent, which puts forward higher requirements for the safety and stability of power grid operation. Power grid equipment, especially large-scale transformer equipment, will inevitably be affected by factors such as electricity, heat, and environment during operation, resulting in damage to equipment performance and a series of vicious accidents such as failures [1]. Therefore, providing high-quality power and ensuring the demand for power supply in urban development is the focus of the authors' research. Fault monitoring and diagnosis are usually the goal of the actual operation of large-scale electrical equipment, and its actual running time is determined through daily monitoring, and research measures are active, as shown in Figure 1. From large electronic equipment to fault detection, basic functions such as data acquisition, measurement, control, prevention, measurement, and detection come in handy and advanced functions

such as spontaneity, time support, etc. Automatic power control, intelligent modification, online analysis and decision-making, and integration improve the stable operation and safety of large transformer equipment; therefore, the online monitoring and fault diagnosis system is an important factor to measure the intelligence level of the power grid [2].

2. Literature Review

Fan and Sharma proposed a transformer online monitoring system, which includes electronic components such as transformers and sensors, which can be used to collect and sample voltage parameters in the power grid, the online monitoring system will also collect the collected data, the data is converted into digital signals, and the unified processing of information is completed [3]. In the monitoring process, the system will use CPLD to complete the processing of the sampled data and conduct simulation experiments to verify the data collected in the circuit and obtain ideal

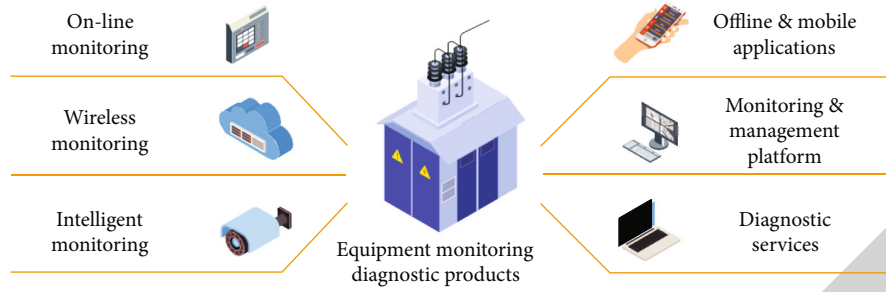


FIGURE 1: Condition monitoring and fault diagnosis system.

monitoring results. This transformer online monitoring system cannot monitor the working environment of the transformer; therefore, the monitoring scope of the system is limited and cannot be applied and promoted in practice. Liu et al. applied the ARM processor to the online monitoring technology of gas in transformer oil and collected the electrical characteristics in the power grid; the online monitoring system can also process the collected data and complete the remote data transmission [4]. The online monitoring technology they designed has strong practicability, but the online monitoring system they designed does not include the factors that affect the parameters of the power grid; that is, the transformer fault cannot be diagnosed. Chakraborty et al. mainly studied the key technology in the intelligent detection technology of distribution transformers, verified the function of the key technology, and obtained the verification results [5]. The detection technology they designed can be used to collect electric energy information in the power grid, the main method is to install current and voltage transformers in distribution transformers, the transformers can collect electric energy information and temperature information in distribution transformers, and all this information is sent to the central server. In the transformer intelligent detection system they established, it can comprehensively collect various parameters of distribution transformers and complete the comprehensive analysis of these parameters, which has certain use value. However, in their system, only uncomplicated nonelectrical parameters can be comprehensively analyzed, and various data cannot fully demonstrate the characteristics of the transformer. The authors describe the use of a data-driven algorithm that can be used in power data reception systems as a measurement theory for distribution transformer data reception and maintenance. With the support of the electronic data acquisition system, a total of 96 phase current data instances were used to calculate the Spearman horizontal correlation coefficient and its daily t statistic. Transformer distribution data is recorded by measuring impedance. Finally, the effectiveness of the proposed algorithm is verified by an example analysis.

3. Research Methods

3.1. Anomaly Data Collection Detection Model Using t Statistic. The electronic data collection process of electronic power users is an application for collecting, processing, and

monitoring electronic power information of consumers. The electric energy data acquisition system is used to collect, process, and monitor the power consumption information in real time. According to the procedures, good performance such as automatic collection of electronic data, negative monitoring, good electrical monitoring, electrical inspection and control, data interference, power distribution analysis, and intelligent electronic equipment data exchange can be completed.

The system consists of 3 layers: main layer, communication layer, and device layer [6]. In key processes, functions such as precommunication, application marketing, administration, and data management are seen. In the communication process, many performances of wire and wireless connections are provided to exchange information between the main system and the terminal equipment. The following process of electronic data acquisition system is mainly composed of collector, collection terminal, electricity meter, and concentrator. From bottom to top are the electricity meter, the main electricity meter, and the electrical equipment or accessories that collect electricity consumption data; then, the written data is transmitted to the content through various communication technologies; finally, the recorded data is stored in different servers analyzed on. This is done on a workbench from which the operator can monitor work conditions and measurements.

Facilitate the collection, export, and processing of electronic data processing systems with energy-efficient electronic processing data that can be used for problem solving and evaluation [7]. In modern electronic data acquisition systems, the current size of each consumer electronics is typically sampled 96 times a day. Based on the traditional operation and data acquisition, the three-phase current is related, so the correlation coefficient can be used to monitor the negative state of the power user. Do not share data exchanges. The most commonly used are the Pearson coefficient and the Spearman coefficient. For the Pearson correlation coefficient, the sample data requires a Gaussian distribution, but the current data do not follow this classification. The Spearman rank correlation coefficient overcomes this limitation and can be used to identify fragmented and unidentifiable big data [8]. Therefore, the authors adopt Spearman's rank correlation coefficient to express the correlation between three-phase currents. Suppose $I_A = [I_{A1}, I_{A2}, \dots, I_{AN}]^T$, $I_B = [I_{B1}, I_{B2}, \dots, I_{BN}]^T$, and $I_C = [I_{C1}, I_{C2}, \dots, I_{CN}]^T$ are the current sampling data of phase A, B, and C for one day,

respectively. Sort the elements in each vector from largest to smallest, so the matrix vector composed of I_A , I_B and I_C can be obtained as

$$I_{ABC}^R = \begin{bmatrix} I_{A1}^R & I_{A2}^R & \cdots & I_{AN}^R \\ I_{B1}^R & I_{B2}^R & \cdots & I_{BN}^R \\ I_{C1}^R & I_{C2}^R & \cdots & I_{CN}^R \end{bmatrix}. \quad (1)$$

In formula (1), N represents the window length of each detection. Before determining Spearman's rank correlation coefficient, the ranking matrix should first be normalized, convert the matrix I_{ABC}^R to I_{ABC}^{R*} to better display the difference between the three-phase currents, and the elements of I_{ABC}^{R*} can be obtained as

$$I_{ABC,ij}^{R*} = \frac{I_{ABC,ij}^R - 1/N \sum_{j=1}^N I_{ABC,ij}^R}{\sqrt{1/N - 1 \sum_{j=1}^N \left(I_{ABC,ij}^R - 1/N \sum_{j=1}^N I_{ABC,ij}^R \right)^2}}. \quad (2)$$

Define the Spearman rank correlation coefficient matrix corresponding to the three-phase current as

$$\rho^S = \begin{bmatrix} \rho_{AA}^S & \rho_{AB}^S & \rho_{AC}^S \\ \rho_{BA}^S & \rho_{BB}^S & \rho_{BC}^S \\ \rho_{CA}^S & \rho_{CB}^S & \rho_{CC}^S \end{bmatrix}, \quad (3)$$

$$\rho_{XY}^S = \frac{\sum_{j=1}^N \left(I_{ABC,Xj}^{R*} - \overline{I_{ABC,X}^{R*}} \right) \left(I_{ABC,Yj}^{R*} - \overline{I_{ABC,Y}^{R*}} \right)}{\sqrt{\sum_{j=1}^N \left(I_{ABC,Xj}^{R*} - \overline{I_{ABC,X}^{R*}} \right)^2} \sqrt{\sum_{j=1}^N \left(I_{ABC,Yj}^{R*} - \overline{I_{ABC,Y}^{R*}} \right)^2}}. \quad (4)$$

In formulas (3) and (4), $X, Y \in \{A, B, C\}$, $X \neq Y$, $\overline{I_{ABC,X}^{R*}}$ and $\overline{I_{ABC,Y}^{R*}}$ are the averages of vectors $I_{ABC,X}^{R*}$ and $I_{ABC,Y}^{R*}$, respectively. If none of the column vectors I_A , I_B , and I_C has the same value, the value of I_{ABC}^{R*} will be an integer [9]. Equation (4) can be simplified as

$$\rho_{XY}^S = 1 - \frac{6 \sum_{j=1}^N \left(\gamma_j^* \right)^2}{N(N^2 - 1)}. \quad (5)$$

In formula (5), $\gamma_j^* = I_{ABC,Xj}^{R*} - I_{ABC,Yj}^{R*}$, and $\rho_{XY}^S \in [-1, 1]$; the larger the value, the higher the correlation of the phase current. Under the normal operation of the transformer, there is a positive correlation between the three-phase currents; therefore, a larger value means that the distribution transformer has a high probability of maintaining normal operation. If the value is close to 0 or even negative, it means the switch works differently [10]. However, it is difficult to be sure that the value is not close to 1 or 0, and no conclusive results can be obtained from the correlation coefficient. Therefore, sentiment analysis based on statistical research

can be used to judge whether the written data of electronic devices is abnormal [11]. In other words, determine whether the value of ρ_{XY}^S is significantly different from zero. Therefore, the null hypothesis (i.e., $H_0: \rho_{XY}^S = 0$) and the alternative hypothesis (i.e., $H_1: \rho_{XY}^S \neq 0$) are given separately, and a permutation test is used to determine which hypothesis should be accepted. This test takes into account the amount of data in the sample, and the risk of directly using rank correlation coefficients obtained from sample data is avoided [12]. Therefore, issues related to confidence intervals and hypothesis testing are handled using the Fisher transform. The Fisher transform and Z value of ρ_{XY}^S can be defined as equations (6) and (7), respectively:

$$F(\rho_{XY}^S) = \arctan h(\rho_{XY}^S) = \frac{1}{2} \ln \frac{1 + \rho_{XY}^S}{1 - \rho_{XY}^S}, \quad (6)$$

$$z_{XX}^S = \sqrt{\frac{N-3}{1.06}} F(\rho_{XY}^S). \quad (7)$$

In formulas (6) and (7), z_{XX}^S follows a normal distribution. In order to quickly monitor and detect abnormal conditions of transformers in time, only 96 sampling data are usually used for analysis, and accurate monitoring results can be obtained every day [13]. According to statistical theory, when the number of sampled data is large (i.e., >120), a normal distribution will give good results, while results from small sampled data will be good by using the t distribution and the t statistic [14]. The t statistic of the Spearman rank correlation coefficient can be expressed as

$$t_{XY}^S = \rho_{XY}^S \sqrt{\frac{N-2}{1 - \rho_{XY}^S{}^2}}. \quad (8)$$

In equation (8), the t distribution of t_{XY}^S should have degrees of freedom equal to $N-2$. The probability density function of the t distribution is as follows:

$$f(x, n) = \frac{\Gamma[(n+1)/2]}{\sqrt{n\pi}\Gamma(n/2)} \left(1 + \frac{x^2}{n} \right)^{-(n+1)/2}, \quad (9)$$

$$\Gamma(n) = \int_0^{+\infty} x^{n-1} e^{-x} dx. \quad (10)$$

In equations (9) and (10), n is the degree of freedom of the t distribution. The t distribution probability density function is used to determine the thresholds for hypothesis testing of the t statistics shown in Figure 2; i.e., $t_\alpha(N-2)$ is the threshold with significance level equal to α and degrees of freedom equal to $N-2$, which can be derived from equation (9).

$$\int_{t_\alpha(N-2)}^{+\infty} f_t(x, N-2) = \alpha. \quad (11)$$

The curve in Figure 2 is the composite speed and independence of the T -division function, and the shaded area represents the infinite $f_t(x, N-2)$ of $t_\alpha(N-2)$. Therefore, given

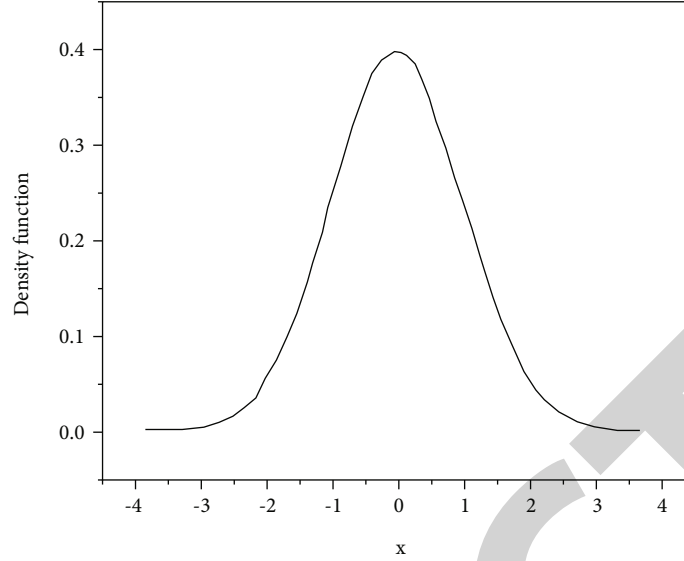


FIGURE 2: Probability density function of t distribution with significance level equal to α and degrees of freedom equal to $N - 2$.

the values for level α and the independent level, it is possible to detect differences in the distribution of electronic devices by making assumptions using the t statistic. If $\alpha = 0.05$ and $N = 96$, then $t_{\alpha}(N - 2) = 1.661$. The steps of abnormal data collection and detection are as follows: (1) obtain Spearman's rank correlation coefficient ρ_{XY}^S and the corresponding t statistic t_{XY}^S of the three-phase current; (2) if $t_{XY}^S < 0$, determine that the transformer is in an abnormal state, and go to step (5); otherwise, go to step (3); (3) establish the null hypothesis $H_0: \rho_{XY}^S = 0$ and the alternative hypothesis $H_1: \rho_{XY}^S \neq 0$; select the significance level $\alpha = 0.05$, which is the most commonly used value in hypothesis testing; (4) calculate t_{XY}^S and compare it with $t_{\alpha}(N - 2)$ [15]. If $t_{XY}^S \geq t_{\alpha}(N - 2)$, reject H_0 , indicating that the transformer is in a normal input state; otherwise, accept H_0 ; that is, the transformer is in an abnormal state; and (5) update the data window and return to step (1). Conceptual data-driven algorithms can be used to power a real power user data receiving system, the data flow of which is shown in Figure 3.

In Figure 3, there are 3 standard ways to monitor abnormal data acquisition, namely, (1) $\rho_{XY}^S < 0$, (2) $t_{XY}^S < 0$, and (3) $t_{XY}^S \leq t_{\alpha}(N - 2)$. Criteria (1) and (2) only make sense when electrical reversal or reverse connection occurs. t_{XY}^S may be small but positive when there is power theft, three-phase unbalance, or other unknown anomalies, so in this case, criterion (3) is meaningful. Therefore, these 3 criteria are for different abnormal situations.

4. Analysis of Results

4.1. The Basis of the Example. Examples presented are data on electrical power distribution to identify the effectiveness of data-driven analysis algorithms for data acquisition. In it, the electronic power supply receives the system, instantaneous active and reactive power, three- or two-phase cur-

rent, and voltage amplitudes, and all power types are closed [16]. In these measurements, it is difficult to apply the current power or power values to determine whether the input voltage of the transformer is normal, and the fluctuation of phase voltage is usually small. Therefore, the phase current is used to detect the data acquisition status of the distribution transformer. A total of 9 scenarios are set in the calculation example, including 8 abnormal data acquisition scenarios and 1 normal data acquisition scenario.

4.2. Comparative Analysis. Scenario 1 (representing abnormal data acquisition scenario) and scenario 9 (representing normal data acquisition scenario) are, respectively, selected to illustrate the proposed algorithm. For scenario 1, scenario 1 has large phase current fluctuations from 2021-04-01T00:00 to 2021-05-31T23:45. There are 3 concave positions in the Spearman rank correlation coefficients of currents between different phases, so it is suspected that abnormal data collection occurred in 2021-04-04, 2021-04-30, and 2021-05-11. However, if only the Spearman rank correlation coefficient is used, a certain threshold cannot be given to determine [17]. Therefore, the t statistic is added. The value of t_{BC}^S exceeded the threshold in 2021-04-30 and returned to normal in 2021-05-01. Therefore, two different types of alarms were triggered on 2021-04-04 and 2021-04-30, respectively, indicating that abnormal data is highly likely to be acquired in phase B and cleared after maintenance. Therefore, the proposed algorithm can detect abnormal data of distribution transformers and remind maintenance personnel to check them in time. The value of t_{CA}^S for 2021-04-04 exceeds the threshold but is still positive [18]. Therefore, while it is possible to detect abnormal behavior in the BC phase based on a negative t statistic, abnormal behavior in the CA phase cannot be detected if the detection criterion is based only on the sign of the t statistic. That is, the threshold $[t_{\alpha}(N - 2)]$ cannot be set too large. If the set threshold is larger, the false alarm of AB phase will be triggered

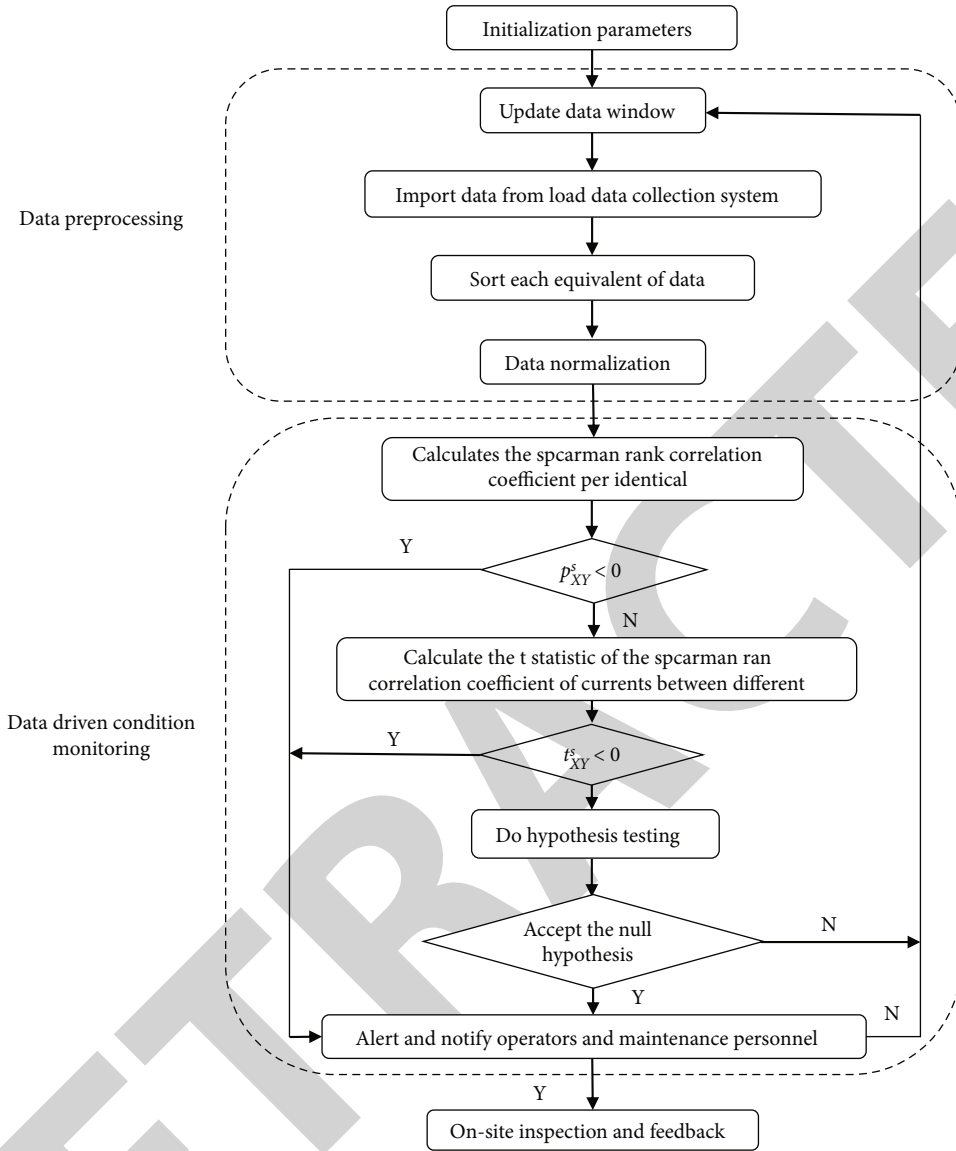


FIGURE 3: Algorithm flow chart of condition monitoring.

TABLE 1: Abnormal data collection results in 8 scenarios.

Scenes	Time limit	1st alarm	Alarm phase	Maintenance time
1	[2021-04-04, 2021-05-31]	2021-04-04	BC, CA	2021-04-06
		2021-04-30	BC	2021-05-01
2	[2021-06-20, 2021-07-27]	2021-06-29	CA	2021-06-30
3	[2020-05-17, 2021-06-10]	2020-05-29	BC, CA	2020-06-06
4	[2020-09-01, 2021-06-23]	2020-09-10	CA	2020-09-30
5	[2020-09-01, 2020-11-10]	2020-09-25	AB, CA	2020-10-28
6	[2020-10-01, 2021-01-01]	2020-10-01	AB, CA	2020-10-29
7	[2020-10-01, 2020-11-30]	2020-10-01	AB, CA	2020-10-29
8	[2020-12-01, 2021-01-31]	2020-12-01	CA	2021-01-03

in 2021-04-04, and the false alarm of AB and CA phase will be triggered in 2021-04-30. Therefore, an appropriate threshold should be determined according to statistical theory. The parameters in the threshold determination are the significance level (α) and the sampling rate (N), and their values will affect anomaly detection. The results of the other seven abnormal data collection scenarios are shown in Table 1. For scenarios 2-8, only one alarm was triggered during operation, and it was all cleared after maintenance. The result shows that the algorithm can successfully detect abnormal data collection of distribution transformers. Generally, whenever a transformer is suspected of being abnormal, an on-site inspection and overhaul of the transformer should be performed. On-site inspections and inspections are carried out by maintenance personnel from the power company and include procedures for checking oil temperature, oil leaks, noise, moisture, pressure, and electrical wiring [19].

To further illustrate the characteristics of traditional data collection, scenario 9 is used to describe the detailed search process of the algorithm.

As can be seen, I_A , I_B , and I_C fluctuate synchronously, and their Spearman rank correlation coefficients are very close to 1. Therefore, there is a relationship of three-phase currents, and it can be considered that the transformer in scenario 9 is in a normal data state. Neither t_{AB}^S nor t_{AC}^S , t_{BC}^S exceeds the threshold, and the curves of all t statistics are far from the threshold line [20]. Therefore, it can be concluded that in scenario 9, no abnormal data collection occurs in the distribution transformer.

4.3. Scheme Sensitivity Analysis

4.3.1. Sensitivity Analysis of Different Significance Levels. To discuss the effect of significance at level α on the variance of the monitoring data, sensitive observations were made for several key levels (0.0005, 0.001, 0.005, 0.01, 0.05, and 0.1) for scenarios 1-8. Table 2 shows the time to first alarm for different key stages of scenarios 1-8.

As can be seen from Table 2, for scenarios 4-8, the results do not change with α change, which means that scenarios 4-8 are not sensitive to the significance level. However, for scenarios 1 and 2, if α is set to be large, the alert will hardly be triggered and the potential anomaly may be ignored. For scenario 3, if the value of α is set smaller, more alarms will be triggered. Also, in scenarios 1 and 3, there is some small drift in the first alarm time. In scenario 1, when α is set to [0.0005, 0.001] and [0.005, 0.05], the results are relatively insensitive to the significance level. In scenario 2, when α is set to [0.0005, 0.05], the result is relatively insensitive. In Scenario 3, when α is set to [0.005, 0.01], the result is relatively insensitive. Therefore, intersecting the insensitive ranges of scenarios 1-8, it can be concluded that the insensitive interval to the significance level is [0.005, 0.05]. Therefore, in practical applications, any value can be selected within the insensitive interval for the significance level of the algorithm.

4.3.2. Sensitivity Analysis of Different Sampling Rates. As mentioned above, electronic data loggers collect and store data 96 times a day. However, in some appliances, the data

TABLE 2: The first alarm time of each scenario under different significance levels.

Scenes	Years	Significance level					
		0.0005	0.001	0.005	0.01	0.05	0.1
1	2021	04-04	04-04	04-04	04-04	04-04	04-04
		04-29	04-29	04-30	04-30	04-30	
2	2021	06-29	06-29	06-29	06-29	06-29	—
		05-28					
3	2020	05-31	05-28	05-29	05-29	05-29	05-29
		06-05	05-31				
4	2020	09-10	09-10	09-10	09-10	09-10	09-10
5	2020	09-25	09-25	09-25	09-25	09-25	09-25
6	2020	10-01	10-01	10-01	10-01	10-01	10-01
7	2020	10-01	10-01	10-01	10-01	10-01	10-01
8	2020	12-01	12-01	12-01	12-01	12-01	12-01

TABLE 3: The maximum absolute difference of each scene under different sampling rates.

Scenes	Sampling rate		
	96/day	48/day	24/day
1	4.1423	4.2663	3.1155
2	1.8726	1.9991	2.1676
3	1.0108	0.9231	1.7181
4	1.6610	1.6790	1.7170
5	11.2620	8.3544	6.2872
6	225.9900	130.4500	81.1430
7	36.5910	28.0720	19.7540
8	36.5900	28.0710	19.7520

is only checked 24 or 48 times a day. In order to demonstrate the effectiveness of the applied algorithm in different power systems and under different conditions, sensitivity tests were performed on different models, and the difference value (i.e., $t_{XY}^S - t_\alpha(N-2)$) when the transformer was in abnormal state was obtained, and the calculation results are shown in Table 3. The greater the difference between each line, the stronger the algorithm using the measurement model. As can be seen from Table 3, with 96 samples per day, 5 cases (e.g., scenarios 4-8) get the highest value, indicating a higher ratio; otherwise, the transition is better [21]. Therefore, a higher ratio is recommended. Furthermore, it can be seen that the change in the largest difference was not very large and did not change the benefits of care. Therefore, it can be determined that the change in design will not have a significant impact for most of the 24 or 48 time period, which means that the design process can be effectively used to strike dynamics.

The algorithm is used for the actual electronic grid, and the abnormal data have been carefully examined and validated. The unique steps of implementing the concept are as follows: tsis negative inspection, ua preinspection, chaw site inspection, and kaw closed loop control. In step (1),

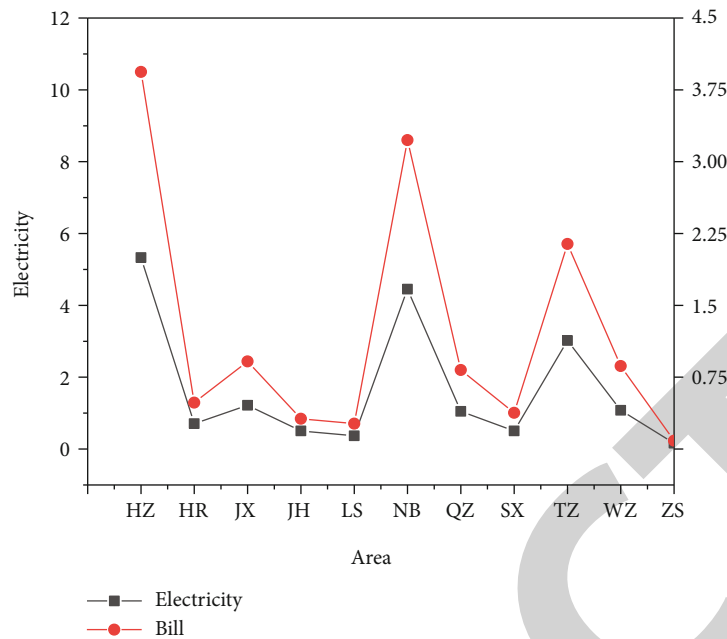


FIGURE 4: Electricity charge recovery bills for each regional subsystem of the power system.

administrators use process planning to perform oracle database-based anomaly data collection detection. In step (2), unreliable users are prescreened to improve authentication. In step (3), the Department of Labor will work with relevant agencies to assess the location of negative user changes. In step (4), the recovery of electricity bills will be followed up [22]. The algorithm is applied to 11 regional subsystems (HZ, HR, JX, JH, LS, NB, QZ, SX, TZ, WZ, and ZS) on the power grid, and the recovery rate of each region is shown in Figure 4.

In Figure 4, the numbers on the left ordinate and bar graph represent power returns, respectively, while the numbers on the right ordinate and black line graph represent the values returned by each subsystem. It can be seen that the renewable income is the largest (3.951 million yuan, 5300 MWh) and the lowest renewable income (038,400 yuan, 52 MWh). After the algorithm was used, 136 users recovered a total of 12.98 million yuan from the grid and consumed 17.57GWh of electricity, proving the efficiency of the algorithm.

5. Conclusion

The authors propose a data-driven monitoring algorithm for abnormal data acquisition of distribution transformers based on t statistics. Through the study of the actual scene and the corresponding sensitivity analysis, the feasibility of the proposed algorithm is proved; by using this algorithm, abnormal data of distribution transformers can be detected more accurately; and in time, thus, a lot of manpower and financial resources are saved, so it can be well used for abnormal data collection and detection of distribution transformers in practical applications.

Data Availability

The data used to support the findings of this study are available from the corresponding author upon request.

Conflicts of Interest

The authors declare that they have no conflicts of interest.

References

- [1] S. H. Kim and H. B. Lee, "Impact stray load loss on distribution transformer depending on material of clamp and tank," *Transactions of the Korean Institute of Electrical Engineers*, vol. 69, no. 2, pp. 265–270, 2020.
- [2] S. H. Kim and H. B. Lee, "Optimum design of core for loss reduction of shell type distribution transformer," *Transactions of the Korean Institute of Electrical Engineers*, vol. 69, no. 3, pp. 414–418, 2020.
- [3] M. Fan and A. Sharma, "Design and implementation of construction cost prediction model based on SVM and LSSVM in industries 4.0," *International journal of intelligent computing and cybernetics*, vol. 14, no. 2, pp. 145–157, 2021.
- [4] Y. Liu, D. Liang, Y. Wang, P. Kou, and C. Yang, "Power flow analysis and DC-link voltage control of hybrid distribution transformer," *IEEE Transactions on Power Electronics*, vol. 36, no. 11, pp. 12579–12595, 2021.
- [5] S. Chakraborty, S. Jain, A. Nandy, and G. Venture, "Pathological gait detection based on multiple regression models using unobtrusive sensing technology," *Journal of Signal Processing Systems*, vol. 93, no. 1, pp. 1–10, 2021.
- [6] S. Liu, Y. Zhao, Z. Lin et al., "Data-driven condition monitoring of data acquisition for consumers' transformers in actual distribution systems using t -statistics," *IEEE Transactions on Power Delivery*, vol. 34, no. 4, pp. 1578–1587, 2019.

- [7] S. Tacoma, B. Heeren, J. Jeuring, and P. Drijvers, "Intelligent feedback on hypothesis testing," *International Journal of Artificial Intelligence in Education*, vol. 30, no. 4, pp. 616–636, 2020.
- [8] D. Liu, H. Zhen, D. Kong, X. Chen, and H. Wang, "Sensors anomaly detection of industrial internet of things based on isolated forest algorithm and data compression," *Scientific Programming*, vol. 2021, no. 1, 9 pages, 2021.
- [9] Z. Jadidi, E. Foo, M. Hussain, and C. Fidge, "Automated detection-in-depth in industrial control systems," *The International Journal of Advanced Manufacturing Technology*, vol. 118, no. 7-8, pp. 2467–2479, 2022.
- [10] M. Bradha, N. Balakrishnan, A. Suvitha et al., "Experimental, computational analysis of butein and lanceoletin for natural dye-sensitized solar cells and stabilizing efficiency by IoT," *Environment, Development and Sustainability*, vol. 24, no. 6, pp. 8807–8822, 2022.
- [11] Y. Pan, X. Zhao, Z. Xu, J. Li, and L. Liu, "Research on abnormal behavior recognition of buses based on improved support vector machine," *Journal of Advanced Transportation*, vol. 2021, no. 1, 8 pages, 2021.
- [12] G. Garate, I. Harismendy, O. Echeverria-Altuna, and J. Estévez, "A dynamic data driven application system for real-time simulation of resin transfer moulding processes," *International Journal of Material Forming*, vol. 15, no. 3, pp. 1–11, 2022.
- [13] J. Alves, D. Castonguay, and T. Brüstle, "Unit form recognition by mutations: application of mutations in the search of positive roots," *Discrete Applied Mathematics*, vol. 291, no. 4, pp. 223–236, 2021.
- [14] L. Zhang and M. Leach, "Evaluate the impact of sensor accuracy on model performance in data-driven building fault detection and diagnostics using Monte Carlo simulation," *Building Simulation*, vol. 15, no. 5, pp. 769–778, 2022.
- [15] J. Chen, J. Liu, X. Liu, X. Xu, and F. Zhong, "Decomposition of toluene with a combined plasma photolysis (cpp) reactor: influence of UV irradiation and byproduct analysis," *Plasma Chemistry and Plasma Processing*, vol. 41, no. 1, pp. 409–420, 2021.
- [16] T. H. Lye, R. Roshankhah, Y. Karbalaieisadegh, S. A. Montgomery, and J. Mamou, "In vivo assessment of pulmonary fibrosis and edema in rodents using the backscatter coefficient and envelope statistics," *The Journal of the Acoustical Society of America*, vol. 150, no. 1, pp. 183–192, 2021.
- [17] J. U. Woo, M. Kim, J. Rhie, and T. S. Kang, "Aftershock sequence and statistics of the 2017 mw 5.5 Pohang, South Korea, earthquake: implications of fault heterogeneity and postseismic relaxation," *Bulletin of the Seismological Society of America*, vol. 110, no. 5, pp. 2031–2046, 2020.
- [18] R. Huang, S. Zhang, W. Zhang, and X. Yang, "Progress of zinc oxide-based nanocomposites in the textile industry," *IET Collaborative Intelligent Manufacturing*, vol. 3, no. 3, pp. 281–289, 2021.
- [19] K. Han, Y. Duan, R. Jin, Z. Ma, and X. Cai, "Attack detection method based on Bayesian hypothesis testing principle in cps," *Procedia Computer Science*, vol. 187, no. 4, pp. 474–480, 2021.
- [20] F. Farokhi, "Non-stochastic hypothesis testing for privacy," *IET Information Security*, vol. 14, no. 6, pp. 754–763, 2020.
- [21] H. Xie, Y. Wang, Z. Gao, B. Ganthia, and C. Truong, "Research on frequency parameter detection of frequency shifted track circuit based on nonlinear algorithm," *Nonlinear Engineering*, vol. 10, no. 1, pp. 592–599, 2021.
- [22] H. Sun, R. Liu, and C. Gao, "A simplified decoding method of polar codes based on hypothesis testing," *IEEE Communications Letters*, vol. 24, no. 3, pp. 530–533, 2020.